J Mater Cycles Waste Manag (2017) 19:959–967
DOI 10.1007/s10163-016-0499-7

ORIGINAL ARTICLE

Physicochemical properties of slags produced at various amounts of iron addition in lead smelting

Grzegorz Krawiec[1] · Marianna Czaplicka[1] · Jozef Czernecki[1]

Received: 28 April 2015 / Accepted: 29 March 2016 / Published online: 18 April 2016

Abstract In the process of lead production from lead-bearing materials generated in copper metallurgy, a large amount of hazardous waste in the form of slag is produced. To assess the effect of the slag on the environment, its physicochemical properties were determined. In this study, the following methods were used: wavelength dispersive X-ray fluorescence (WD XRF), X-ray diffraction (XRD), and Bunte-Baum-Reerink method to determine softening and melting points, as well as viscosity examination and leaching tests. The measurements were performed on the slag produced with two different amounts of iron addition to the lead smelting process. The resulting slags, an oxide rich phase slag and a sulfide rich phase slag have different compositions and physicochemical properties. It was found that the increase in iron addition causes an increase in the softening melting point of the oxide rich phase slag by about 100 °C, and a twofold increase in the viscosity of both slag phases. The increase in iron addition also results in the decrease in As leachability and increase in Zn, Fe, and Cu leachability from the slags. Slag produced with increased iron addition has a greater impact on the environment.

Keywords Industrial waste · Slag · Characterization · Lead

✉ Grzegorz Krawiec
grzegorz.krawiec@imn.gliwice.pl

Marianna Czaplicka
marianna.czaplicka@imn.gliwice.pl

Jozef Czernecki
jozef.czernecki@imn.gliwice.pl

[1] Institute of Non-Ferrous Metals, Sowinskiego Str. 5, 44-100 Gliwice, Poland

Abbreviations

OPh	Oxide rich phase
SPh	Sulfide rich phase
Series A	Controlled lead smelting with normal iron addition
Series B	Controlled lead smelting with increased iron addition

Introduction

Slag from non-ferrous metal industries is characterized by a very wide range of physicochemical properties, which results from the application of different smelting technologies.

In non-ferrous metal industries, we adjust the slag composition within the FeO_x–SiO_2–CaO system or select other slag systems, for example, soda slag, to achieve a low liquidus temperature and other desired slag properties (e.g., viscosity). The melting point of these slags varies from 600 to 1400 °C [1, 2].

Every type of slag in non-ferrous metal industries creates different problems related to its storage, disposal, and utilization [3–7].

Soda slag is the predominant type of slag in lead metallurgy. When considering the overheated liquid phases (metal and slag), the process temperature is in the 1,000–1,200 °C range [1, 8, 9]. The smelting process is conducted in a reducing atmosphere.

Copper sulfides in the form of such minerals as chalcocite (Cu_2S), bornite (Cu_5FeS_4), covellite (CuS), and chalcopyrite ($CuFeS_2$), are the main components of Polish copper concentrates treated in the smelters [10, 11].

Lead represents the most significant, in terms of mass, metal by-product in the copper-bearing minerals [10–13], and its content in the Polish copper concentrates ranges from 1.5 to 4.0 wt%, depending on the deposit [10].

During the melting of copper concentrates and processing of intermediate products, lead concentrates mainly in dusts and slimes collected in the installations for dedusting the process gases [14–17]. Depending on the applied technology, the lead extracted in the filters or installations for wet dedusting comes in the form of oxide, carbonate, sulfide, or sulfate. These products are directed to reduction processes in rotary–rocking furnaces with the addition of approximately 1 wt% of sodium carbonate and approximately 15 wt% of iron (usually in the form of small iron scrap).

The introduced metallic iron acts as a substrate for a single-displacement reaction. It reacts with the lead sulfide in the charge, and makes precipitation of metallic lead possible, according to the following reaction:

$$PbS + Fe = Pb + FeS \quad (1)$$

Metallic iron also acts as a refining agent and affects the purity of crude lead, i.e., by binding As in Fe_2As and $FeAs_2$, it reduces the arsenic content in crude lead.

After completion of the smelting process, the liquid products are cast into a ladle to separate the lead from the slag and Fe–As alloy. Phase separation during solidification (liquation process) produces two slag layers of different chemical compositions: an oxide rich layer (OPh) and a sulfide rich layer (SPh).

Lead is cast into ingots, while the solidified slag after its separation from the Fe–As alloy can be recycled.

The aim of this study is to present the characteristics, i.e., physicochemical properties, of slags formed during the production of lead from materials generated in copper metallurgy with different levels of iron addition, as well as their impact on the environment.

Experimental

Controlled lead smelting was performed in rotary–rocking furnaces with a standard charge and with two different amounts of iron scrap additions: 3 Mg/melt, i.e., 14 wt% content in the charge—(Series A), and 5 Mg/melt, i.e., 23.5 wt% content in the charge—(Series B).

Slag samples were taken from both phases—the oxide rich (OPh) and sulfide rich (SPh) phase. Then, after crushing and averaging, the samples were subjected to thorough testing following the methods described below.

Analytical methods

Wavelength dispersive X-ray fluorescence

The quantity of the main elements in the slag samples was determined by the X-ray fluorescence spectrometry (WD XRF) with a Rigaku (Japan) wavelength dispersive spectrometer ZSX Primus. Samples for analysis were prepared in the form of pellets with the addition of the $SrCO_3$ internal standard. The quantities were obtained with XRF software containing calibration curves for all elements that were present in the process. The XRF application was calibrated with a series of reference materials chemically similar to the studied slag, produced in the Institute of Non-Ferrous Metals.

X-ray diffraction

X-ray examination of the phase composition was performed with a Seifert-FPM XRD 7 X-ray diffractometer. Characteristic Co Kα radiation and a Fe filter were applied. The analysis covered the Bragg angle range 2Θ from 10° to 100°, which corresponds to an interplanar distance d_{hkl} from 1.027 to 0.1168 nm. Identification of crystalline phases in the sample was done with Seifert software, and PDF-2 catalog data of 2007 provided by ICDD company. The quantitative phase analysis was accomplished using the Rietveld method, using the SiroQuant® Version 3.0 programme.

Bunte-Baum-Reerink method

Determination of the melting and softening points was performed by the Bunte-Baum-Reerink (BB) method. It is a variation of a dilatometric method, in which a pellet, made from the material to be tested, of diameter and height of 20 mm is subjected to a constant pressure of 250 G and heated up at a constant rate. Changes in the sample height are registered throughout the test. The temperature at which the sample reaches 93 % of its initial height corresponds to the softening temperature (T_m), while the melting point (T_t) corresponds to the temperature at which the sample reaches 45 % of its initial height [18].

Slag viscosity examination

Studies into slag viscosity were conducted in an installation composed of a Brookfield Engineering Laboratories, Inc. viscometer LVDV-V+ and a chamber oven F 46 120 CM by Barnstead/Thermolyne Corporation. The installation provides the possibilities to perform viscosity measurements in high-temperature conditions by applying the

rotating cylinder method [19]. The melt temperature measurement is carried out by an EL 18 control thermocouple placed in the furnace chamber. Viscosity measurements were performed with alundum crucibles of diameter 50 mm and height of 100 mm.

The viscosity, softening, and melting points are essential characteristic features of this type of material from the point of view of their further treatment.

Studies into eluates

The leaching test of the slag samples was performed according to the standard [20], which specifies the test parameters for leaching of granular materials and residues. Single-stage leaching of slag samples was carried out in distilled water at a ratio of 10:l of liquid to solid. In the test, the solution was placed inside a barrel-shaped container, and was stirred at a rate of 10 rpm. Mixing was conducted for 24 h, and the produced eluate was filtered through a 0.45-μm membrane filter.

Concentration of such metals as As, Zn, Cu, Pb, and Fe in the eluates was determined by Perkin Elmer inductively coupled plasma optical emission spectrometry (ICP-OES). The chloride concentration was determined by the titration method, and that of sulfates with the gravimetric method. Measurements of the alkalinity of eluates (pH) were performed using the potentiometric method.

Results and discussion

Characteristic of samples

The slag samples, originating from the lead melting step, came in the form of compact material, which was comminuted to study it.

The results of the chemical analysis of the samples are shown in Table 1.

The increase in iron addition in the charge from 14 wt% (Series A) to 23.5 wt% (Series B) resulted in a slag mass increase of about 40 %.

Elemental analysis of the slags showed that they mainly contain lead, iron, zinc, and sulfur compounds. The amount of individual elements fluctuates because of the changes in process conditions (oxide and sulfide phase) and iron addition. In the comparison of the slags produced with the same amount of iron addition, it was found that the oxide rich phase (OPh) has a higher lead, arsenic, and SiO_2 content, and a lower zinc, copper, and iron content than the sulfide rich phase (SPh) (Table 1). Separation of the slag into an oxide rich layer (OPh) and a sulfide rich layer (SPh) results from incomplete gravity separation of such phases as slag, matte, speise and metallic lead, which are produced in the lead melting process during cooling.

Table 1 Content of main slag components [wt%]

	OPh		SPh	
	Series A*	Series B**	Series A	Series B
Pb	14.3	8.5	11.3	5.8
Zn	12.0	12.3	16.5	16.4
Cu	1.7	1.2	2.0	1.4
Fe	23.6	26.0	25.5	33.0
S	19.2	20.8	24.2	27.9
As	2.6	0.9	1.1	0.5
Si	2.7	3.0	1.3	0.7
Ca	1.3	1.4	1.4	0.4
Na	1.1	1.1	0.9	0.8
Cl	2.0	2.8	0.6	0.5

* Iron scrap content 14 % in the charge

** Iron scrap content 23.5 % in the charge

The observed increase in iron content in both phases in Series B (increased iron addition) compared with Series A results from the greater amount of refining agent in the form of metallic iron. In the OPh, it reaches a level of 26 wt%, and in the SPh, it reaches 33 wt%.

Phase composition of samples

Figures 1, 2, 3, 4 show the diffraction patterns of the slag samples, which indicate the angular positions and intensity of diffraction reflections (diffraction lines) from different families of lattice planes. Table 2 summarizes the main phase components of the slag samples.

Analysis of the composition of the samples from the oxide rich phase and the sulfide rich phase showed that their basic component is ferruginous sphalerite (Zn, Fe)S, where the Zn atoms are substituted with Fe atoms without changing the crystalline structure of the compound. The content of ferruginous sphalerite ranges from 23.4 % in the OPh from Series A to 40 % for the SPh with increased refining agent addition (Series B) (Table 2). In the examined samples, Fe_2As, $2FeO{\cdot}SiO_2$, FeS, ZnS, PbS, and metallic Pb were also identified.

When comparing ferruginous sphalerite content in the OPh and SPh for the series produced in the same technological conditions, it can be observed that in each case, it was higher in the sulfide rich phase than in the oxide rich one. Increased iron addition (Series B), however, results in an increase in the content of ferruginous sphalerite in both slag phases. In the case of the OPh, it increased from 23.4 to 30.0 wt%, and in the SPh, it increased from 32.2 to 40.0 wt%.

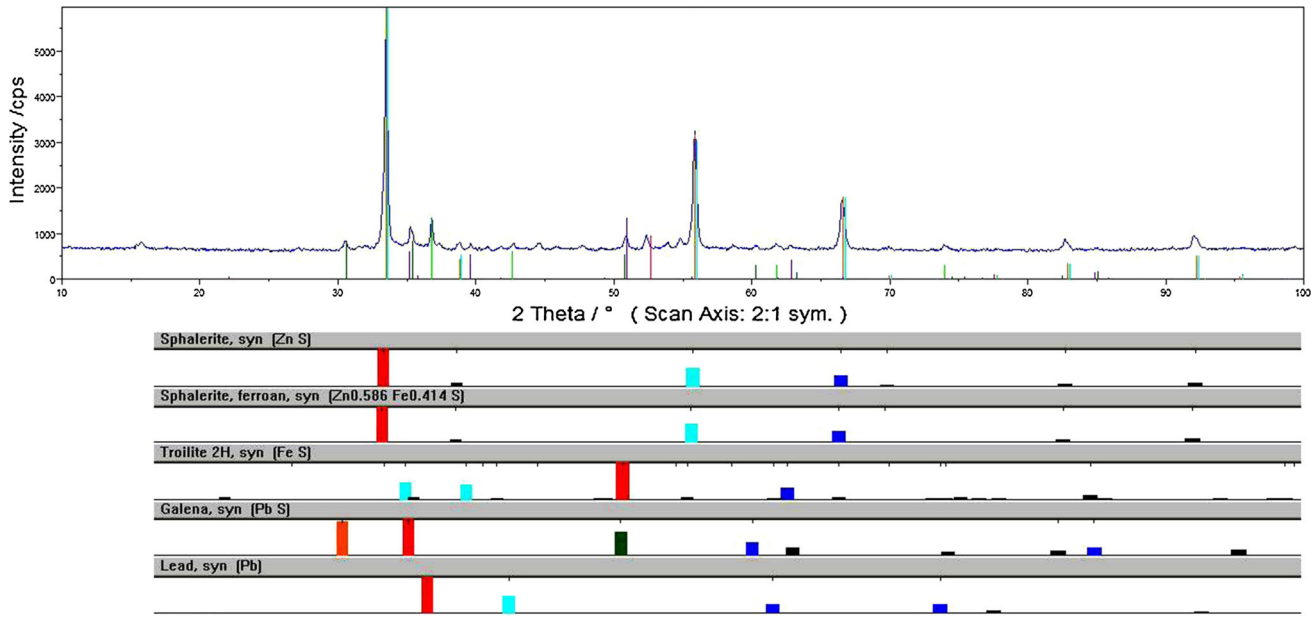

Fig. 1 X-ray pattern of OPh slag sample (Series A)

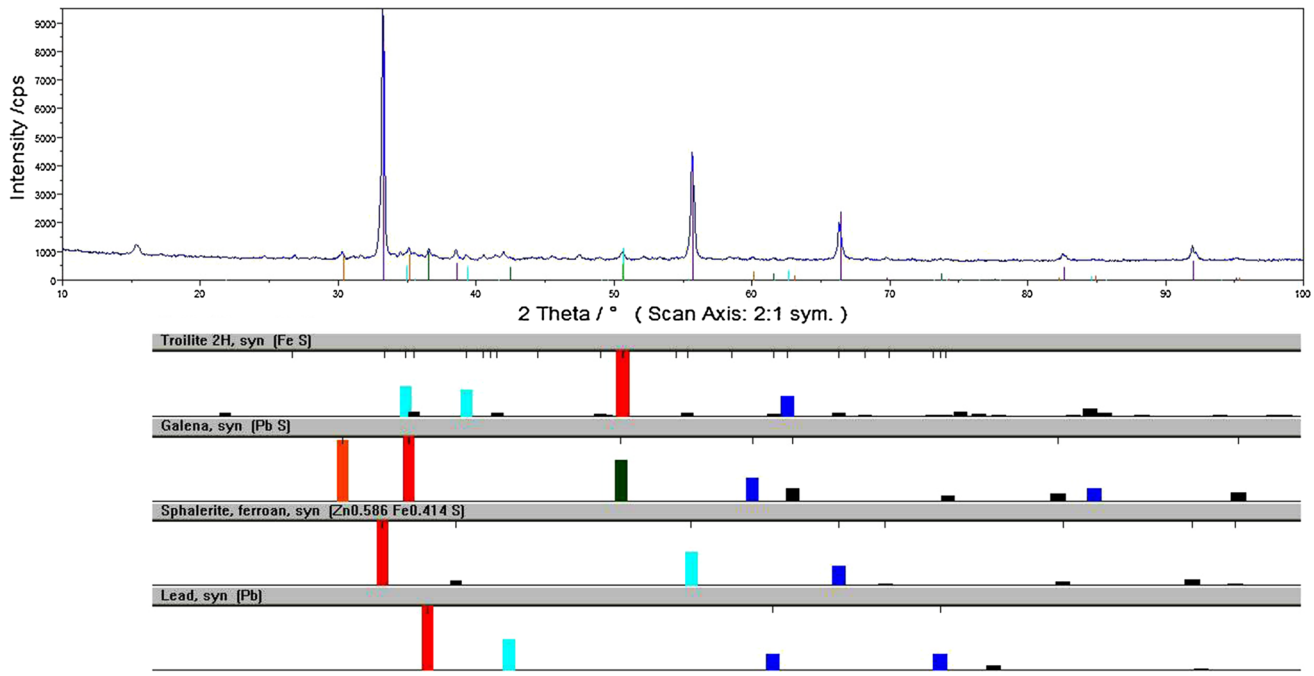

Fig. 2 X-ray pattern of OPh slag sample (Series B)

It was also observed that the increase in ferruginous sphalerite content in both slag phases with the increase in iron addition causes a reduction in ZnS content in both the OPh and SPh.

Another important component in both slag phases is troilite (FeS). Its concentration increased with greater iron addition in both phases: in the OPh from 19.8 to 23.9 wt%, and in the SPh from 25.0 to 35.1 wt%.

Lead in the slag occurs both as PbS and as metallic lead in the form of micro droplets (the XRD method indicated the presence of lead in metallic form). Metallic lead dominates in samples containing less iron, both in the OPh and SPh, while lead sulfide prevails in samples with a larger iron addition. The decrease in the content of both forms of Pb in both slag phases at a higher iron addition results mainly from its dilution (higher slag mass). No new

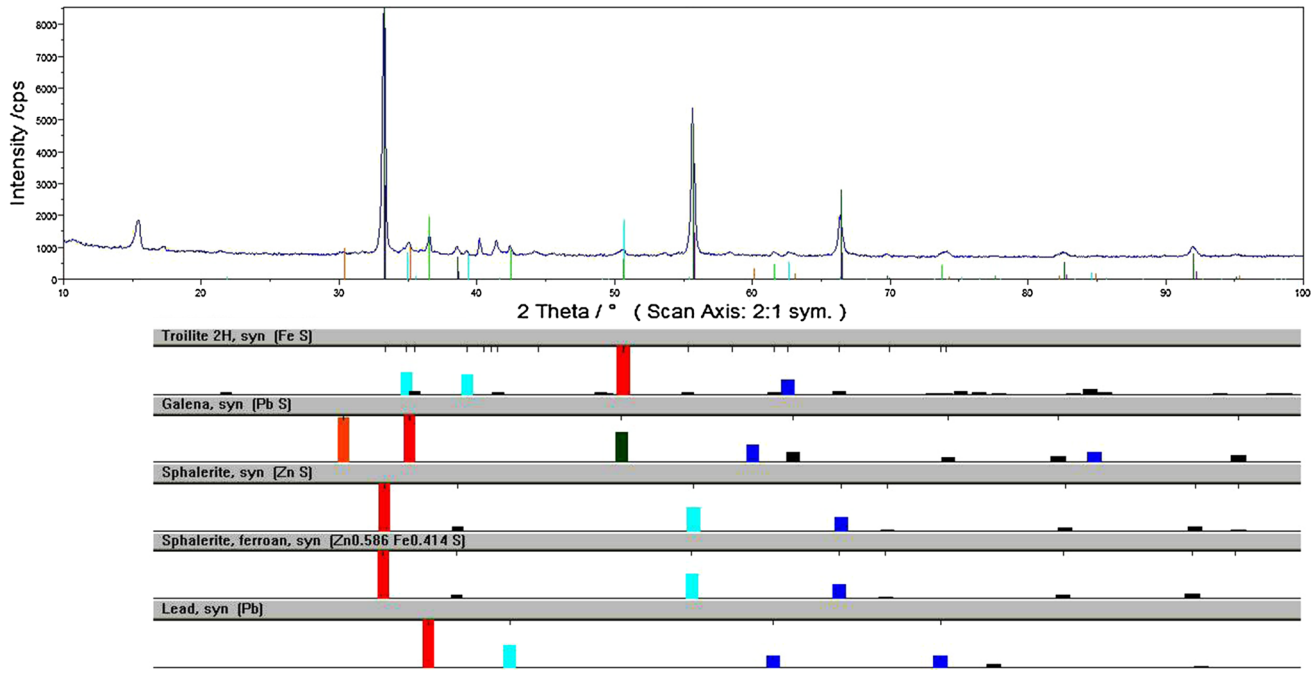

Fig. 3 X-ray pattern of SPh slag sample (Series A)

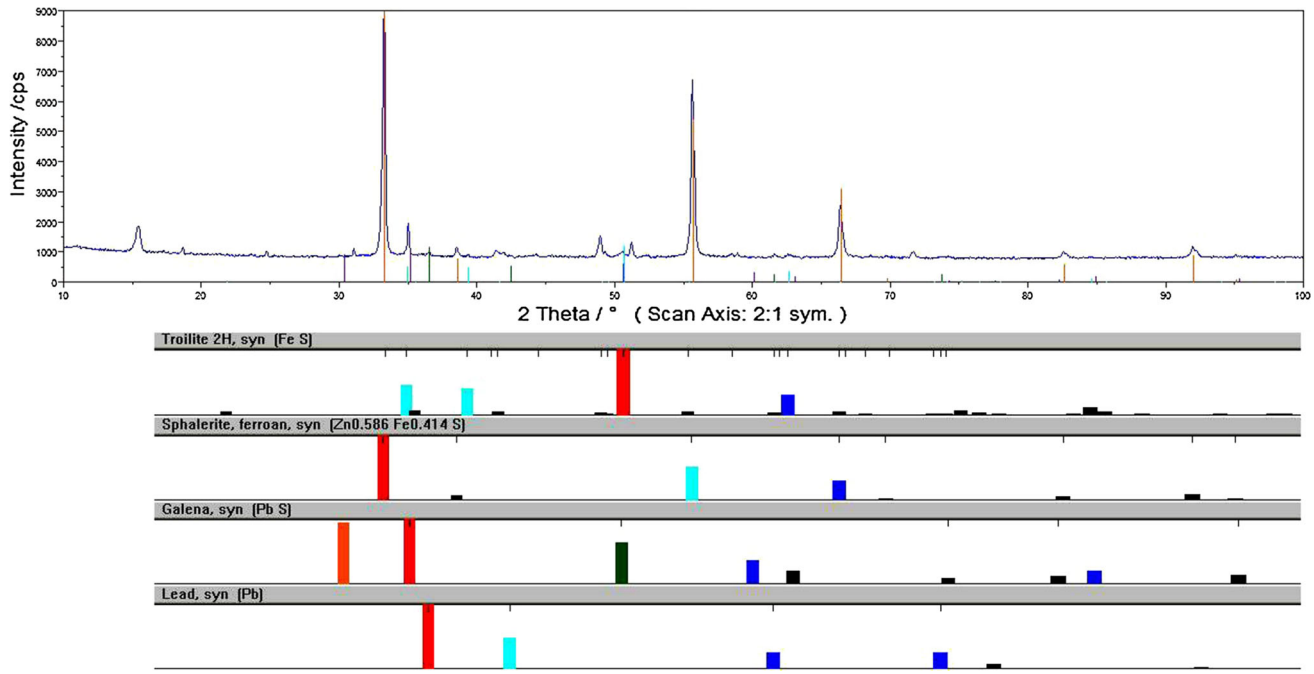

Fig. 4 X-ray pattern of SPh slag sample (Series B)

compounds were observed in the slag after increasing the iron addition to the lead smelting process.

The temperature of both melts was 1,060 °C, and at this temperature, Pb and Zn vaporize. The vaporization of these elements can have some influence on the chemical composition of the slag; however, this influence will be similar for both melts.

The obtained results indicate that the addition of iron has a significant influence on the phase composition of the produced slags.

Table 2 Phase composition of the examined samples [wt %]

	OPh		SPh	
	Series A	Series B	Series A	Series B
Fe_2As	6.4	2.2	2.8	1.3
$2FeO{\cdot}SiO_2$	2.6	3.8	0.0	0.0
$Zn_{0.586}Fe_{0.414}S$	23.4	30.0	32.2	40.0
FeS	19.8	23.9	25.0	35.1
ZnS	3.6	0.0	4.9	0.0
Cu_2S	2.1	1.5	2.5	1.7
PbS	6.9	4.9	5.2	3.5
Pb	8.3	4.2	6.8	2.8

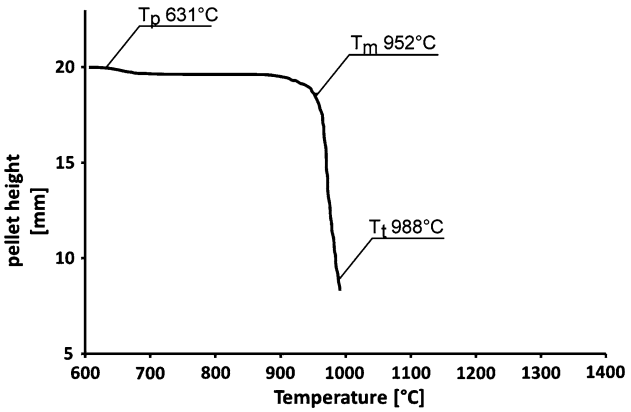

Fig. 5 Measurements of softening and melting points of OPh slag sample (Series A)

Thermal behavior

Results are shown in Figs. 5, 6, 7, 8 and in Table 3.

Studies on the slags showed that the oxide rich phase (OPh) has a lower softening and melting temperature than the sulfide rich phase (SPh) (Table 3). The OPh melts at a temperature of 988 °C, while the SPh melts at 1,092 °C. Increasing the refining agent (metallic iron) addition (Series B) resulted in a change of the slag melting point in both the OPh and SPh, and the softening temperature in the OPh only. The melting point of both phases increased to about 1,160 °C, while the increase in the softening point of the OPh was 76 °C (from 952 to 1,028 °C).

The results of slag viscosity examination are shown in Figs. 9 and 10.

The performed slag viscosity measurements showed that the viscosity of the OPh is higher than the viscosity of the SPh. Above 1,350 °C, there was no significant difference between the viscosities of both phases. An increase in the addition of the refining agent causes a twofold increase in the slag viscosity of both the OPh (Fig. 9) and SPh (Fig. 10) compared with the lower iron addition.

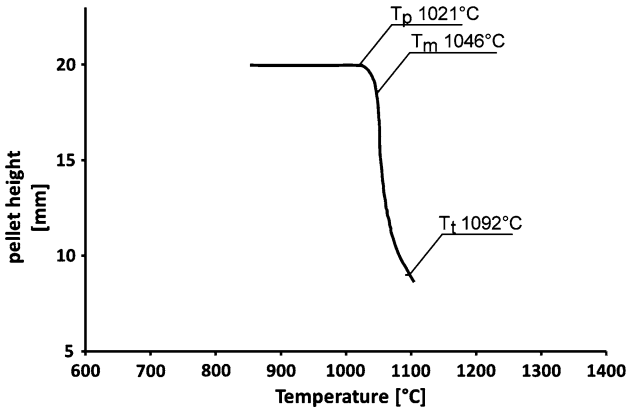

Fig. 6 Measurements of softening and melting points of OPh slag sample (Series B)

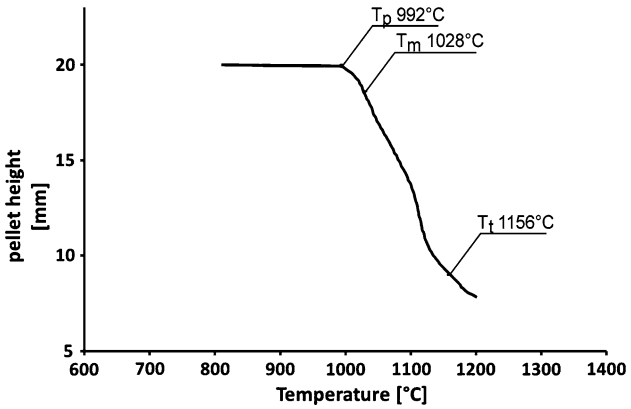

Fig. 7 Measurements of softening and melting points of SPh slag sample (Series A)

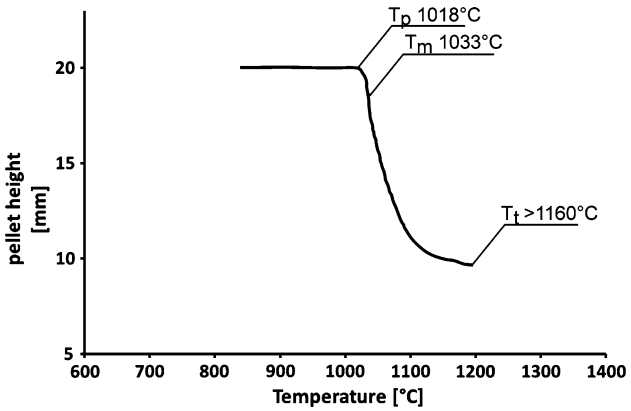

Fig. 8 Measurements of softening and melting points of SPh slag sample (Series B)

Environmental behavior

The results are shown in Tables 4 and 5.

Chemical composition analysis of the eluates showed that they contain As, Zn, Cu, Pb, Fe, Cl^-, and SO_4^{2-}

Table 3 Softening and melting points of the dusts from electric furnace [°C]

	OPh		SPh	
	Series A	Series B	Series A	Series B
Softening start temperature - T_p	631	1,021	992	1,018
Softening point - T_m	952	1,046	1,028	1,033
Melting point - T_t	988	1,092	1,156	>1,160

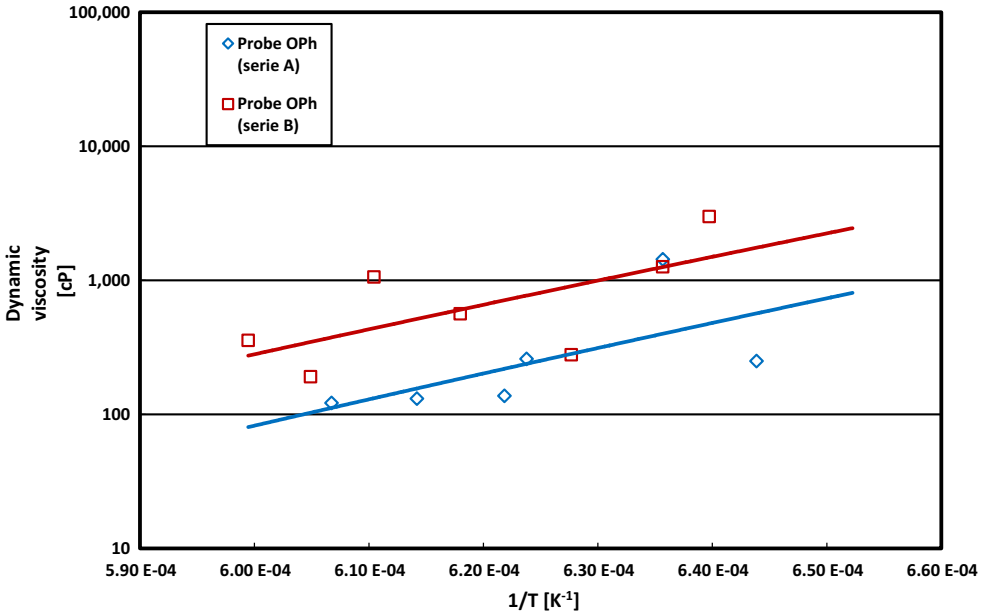

Fig. 9 Results of measurements of viscosity of OPh slag samples

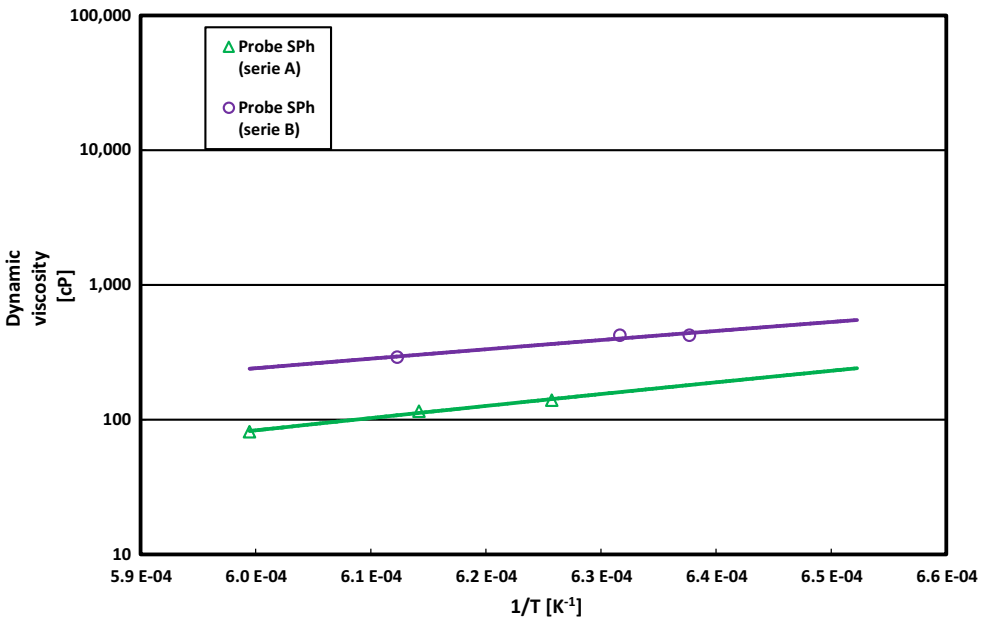

Fig. 10 Results of measurements of viscosity of SPh slag samples

(Table 4). In the process of slag leaching, Cu, Pb, Cl^-, and SO_4^{2-} were eluted from the OPh, and Zn, Cu, Pb, Fe, Cl^-, and SO_4^{2-} from the SPh.

The concentration range of specific elements in the eluate was the following: from the detection limit (Series A OPh) to 1.58 mg/dm^3 (Series B OPh) for Zn; from

Table 4 One step leaching test data for slag [mg/dm^3 of eluate]

	OPh		SPh	
	Series A	Series B	Series A	Series B
As	<0.1	<0.1	2.80	<0.1
Zn	<0.1	1.58	0.28	0.36
Cu	2.06	12.20	0.37	33.30
Pb	0.25	0.56	0.39	<0.1
Fe	<0.1	0.20	0.66	0.80
Cl^-	2,000	2,810	650	520
SO_4^{2-}	820	1,100	140	370

Table 5 One step leaching test other data

	OPh		SPh	
	Series A	Series B	Series A	Series B
pH	9.9	8.3	10.5	9.2
Conductivity [μS/cm]	8,080	10,610	3,720	3,500
Dry residue [g/dm^3]	9.8	11.3	3.2	3.7

0.37 mg/dm^3 (Series A SPh) to 33.3 mg/dm^3 (Series B SPh) for Cu; from the detection limit (Series A OPh) to 0.8 mg/dm^3 (Series B SPh) for Fe; from 520 mg/dm^3 (Series B SPh) to 2,810 mg/dm^3 (Series B OPh) for Cl^-; and from 140 mg/dm^3 (Series A SPh) to 1,100 mg/dm^3 (Series B OPh) for SO_4^{2-} (Table 4).

The results indicate that the OPh slag with increased addition of refining agent (Series B) is the most susceptible to leaching of elements.

The occurrence of As with a 2.8-mg/dm^3 concentration in the eluate from the SPh phase produced with lower iron addition (Series A) confirms the presence of As, which is not bounded with Fe in the slag.

In the case of Zn, Fe, Cu, and SO_4^{2-}, the opposite was observed: the increase in iron addition caused an increase in the concentrations of Fe, Zn, Cu, and SO_4^{2-} in the eluates, for both the OPh and SPh samples. This increase was the most significant in the case of Cu, with its concentration in the eluates from the OPh increasing from 2.1 to 12.2 mg/dm^3, and from 0.4 to 33.3 mg/dm^3 for the SPh.

An increase in Fe in the charge pushes the exchange reaction forward:

$$Cu_2S + Fe = FeS + Cu \quad (2)$$

The formed Cu is transferred to more easily soluble compounds, e.g., $CuSO_4$ and CuCl.

The increase in iron addition causes the concentration of Pb and Cl to increase in the OPh, but decrease in the SPh.

At the end of gravity separation, the slag separates into an oxide rich phase (OPh) and a sulfide rich phase (SPh), since the lighter minerals, e.g., chlorine and oxygen compounds, are present in the oxide rich layer, while the heavier minerals, e.g., sulfur compounds Cu_2S, ZnS, and FeS, are present in the sulfide rich layer. The binding of sulfur with the increased amount of Fe results in binding of additional amounts of Cl in the OPh, which at lower Fe additions would remain in the gaseous phase. Formation of, for example, PbCl in the OPh increases the leachability of Pb and Cl. This is not observed in the SPh due to low levels of Cl.

The eluates from the slag were characterized by a pH ranging from 8.3 for the OPh of Series B to 10.5 for the SPh of Series A. The dry mass of residue ranged from 3.2 g/dm^3 for the SPh of Series A to 11.3 g/dm^3 for the OPh of Series B. The conductivity of eluates varied from 3,500 μS/cm for the SPh of Series B to 10,610 μS/cm for the OPh of Series B (Table 5).

It was found that a greater iron addition causes a decrease in the pH of eluates, regardless of the phase. A decrease in the pH from 9.9 to 8.3 and from 10.5 to 9.2 for the OPh and SPh, respectively, was observed.

The pH and conductivity are strongly influenced by the concentration of Cl^- and SO_4^{-2}. The eluates from the OPh have lower concentrations of Cl^- and SO_4^{-2} compared with the SPh phase (Table 4 and 5).

An influence of the Fe addition on the dry residue in the eluate from both slag phases was also observed: in the case of the OPh, the dry residue mass increased from 9.8 g/dm^3 (Series A) to 11.3 g/dm^3 (Series B), and for the SPh from 3.2 g/dm^3 (Series A) to 3.7 g/dm^3 (Series B). The electrical conductivity of the eluates also changed with the increase in iron addition. In the case of the OPh, the conductivity increased from 8,080 to 10,610 μS/cm, and in the case of the SPh, it decreased from 3,720 to 3,500 μS/cm.

The performed study showed that the slag produced with a greater addition of refining agent has the largest influence on the environment.

Conclusions

Based on the study, it was found that:

- each slag phase produced in the process of lead melting differs from the other both in chemical composition and physicochemical properties,
- the increased addition of iron in the smelting process results in the binding of additional quantities of sulfur and zinc in the slag in the form of ferruginous sphalerite. As a result, the content of sulfur increases both in the oxide rich and sulfide rich phase of the slag,
- an increase in the content of ferruginous sphalerite causes an increase in the softening and melting points

of the OPh by about 100 °C, and a twofold increase of the viscosity of both phases,
- the environmental impact of slags varies and depends on the phase and on the amount of iron addition. The greatest effect can be observed in the OPh with an increased addition of refining agent in the form of metallic iron,
- an increase in iron addition to the process causes an increase in the Zn, Fe, Cu, and SO_4^{2-} content in the examined eluates and decrease in As content.
- Slag produced with an increased refining agent addition has the greatest environmental effect.

Acknowledgments This research was supported jointly by the European Regional Development Fund under the Operational Programme Innovative Economy no POIG.01.03.01-24-019/08-00.

The authors would like to thank MEng Jakub Tyszka for his helpful comments and suggestions during the preparation of this paper.

References

1. Davenport WG, King M, Schlesinger M, Biswas AK (2002) Extractive metallurgy of copper. Elsevier, Oxford, UK. ISBN 0-08-044029-0
2. Sinclair RJ (2009) The extractive metallurgy of lead. Spectrum Series, vol 15. The Australasian Institute of Mining and Metallurgy, Carlton Victoria, Australia. ISBN 978 1 921522 02 4
3. Liu Yuqiang, Peng Ruidong, Ya Xu, Changxin Nai Lu, Dong Junrong Ren (2014) Mechanical behavior of typical hazardous waste and its influence on landfill stability during operation J Mater Cycles. Waste Manag 16:597–607
4. Ettler V, Johan Z, Kribek B, Sebek O, Mihaljevic M (2009) Mineralogy and environmental stability of slags from the Tsumeb smelter Namibia. Appl Geochem 24:1–15
5. Murari K, Siddique R, Jain KK (2015) Use of waste copper slag, a sustainable material. J Mater Cycles Waste Manag 17:13–26
6. Shanmuganathan P, Lakshmipathiraj P, Srikanth S, Nachiappan AL, Sumathy A (2008) Toxicity characterization and long-term stability studies on copper slag from the ISASMELT process. Resour Conserv Recycl 52:601–611
7. Lewis AE, Hugo A (2000) Characterization and batch testing of a secondary lead slag. J S Afr Inst Min Metall 2000:365–370
8. Gregurek D, Reinharter K, Majcenovic C, Wenzlb C, Spanring A (2015) Overview of wear phenomena in lead processing furnaces. J Eur Ceram Soc 35:1683–1698
9. Tarasov AV, Besser AD, Mal'tsev VI, Sorokina VS (2003) Metallurgicheskaya pererabotka vtorichnogo svintsovogo syr'ya (Metallurgical Processing of Secondary Lead) Russian Journal of Applied Chemistry, Vol. 76, No. 11, 2003, pp 1881–1882. Translated from Zhurnal Prikladnoi Khimii, Vol. 76, No. 11, 2003, pp 1932–1933
10. The Monograph of KGHM Polska Miedz SA (2007) CBPM Cuprum, Wrocław
11. Saramak D, Tumidajski T, Skorupska B (2010) Technological and economic strategies for the optimization of Polish electrolytic copper production plants. Miner Eng 23:757–764
12. Sawlowicz Z (2013) REE and their relevance to the development of the Kupferschiefer copper deposit in Poland. Ore Geol Rev 55:176–186
13. Drzymala J, Kapusniak J, Tomasik P (2003) Removal of lead minerals from copper industrial flotation concentrates by xanthate flotation in the presence of dextrin. Int J Miner Process 70:147–155
14. Qiang L, Pinto I, Youcai Z (2014) Sequential stepwise recovery of selected metals from flue dusts of secondary copper smelting. J Clean Prod 84:663–670
15. Palumbo FJ, Marsh RL, Gabler RC (1985) Recovery of Metal Values From Copper Converter Flue Dust. United States Department of the Interior, Bureau of Mines Report of Investigations
16. Czaplicka M, Buzek L (2011) Lead speciation in the dusts emitted from non-ferrous metallurgy processes. Water Air Soil Pollut 218(1):157–163
17. Murari K, Siddique R, Jain KK (2015) Use of waste copper slag, a sustainable material. J Mater Cycles Waste Manage 17(1):13–26
18. Zajaczkowski A, Norwisz J, Botor J (1986) Okreslenie temperatury mieknienia latworedukujacych sie materialow tlenkowych. Rudy Metale 31:275–277
19. Zajaczkowski A, Czernecki J, Botor J (1997) Badanie lepkosci zuzli metalurgicznych. Rudy Metale 42:12–18
20. EN 12457-2 (2003)—Characterisation of waste—leaching—compliance test for leaching of granular waste materials and sludges